PHYSICAL REVIEW A VOLUME 48, NUMBER 6 DECEMBER 1993

Light-beam propagation at planar thin-film nonlinear waveguides

Yuri S. Kivshar*
Institut für Theoretische Physik I, Heinrich-Heine-Universität Düsseldorf, D-4000 Düsseldorf 1, Federal Republic of Germany

Manuel L. Quiroga-Teixeiro
Institute for Electromagnetic Field Theory, Chalmers University of Technology, S-41296 Göteborg, Sweden
(Received 19 April 1993)

The light-beam scattering at a symmetric dielectrical waveguide formed by two interfaces between three nonlinear focusing media is considered analytically and numerically. The problem of beam transmission and reflection is effectively analyzed in the framework of the so-called equivalent-particle theory. It is shown also that the beam scattering may be accompanied by a strong emission of radiation which is not taken into account by the equivalent-particle approximation. Radiative losses of the scattering beam are calculated, and the applicability limits of the equivalent-particle approach are discussed by making a comparison between numerical and analytical results. In particular, it is shown that the incident beam may be *captured* by the thin-film waveguide to form a surface wave due to radiation-induced losses.

PACS number(s): 42.65.−k, 42.79.Gn, 42.82.Et, 42.88.+h

I. INTRODUCTION

As is well known, an interesting application of nonlinear optics is in waveguides where an intensity-dependent refractive index can strongly affect the propagation of the electric field. Many possible applications have been suggested, including all-optical devices such as switchers, scanners, limiters and thresholders, modulators, and bistable logic elements. In the case of large nonlinear index changes, the field structure is mostly determined by the intensity-dependent contribution to the refractive index, and this nonlinear feedback can lead to a rich set of phenomena. One of the important effects is self-localization of beams which leads to formation of finite-width self-focused channels, as well as to creation of new types of stationary nonlinear guided and surface waves in thin-film planar waveguides and at dielectric interfaces (see, e.g., the recent review papers [1, 2], and references therein). As was recently shown by Aceves, Moloney, and Newell [3], the propagation of a self-trapped monochromatic cw light beam at an oblique angle of incidence to one or more interfaces separating self-focusing nonlinear media could be reduced to the study of the motion of an equivalent particle in an effective potential for certain well-defined physical limits. It was established that many of the numerical observations (e.g., numerical simulations of the Gaussian beam incidence at the interface separating linear and nonlinear dielectric media [4]) could be qualitatively understood in the context of this equivalent particle theory. One of the important examples is a possibility to explain a bifurcation behavior of a symmetric thin-film waveguide as the power in the guided wave is gradually increased, the effect being predicted in Ref. [5]. The problem with a linear guided layer was considered numerically by Mitchel and Moloney [6], who characterized their numerical results in terms of the equivalent particle approach.

The equivalent-particle theory replaces the problem of a finite-width self-focusing channel by much simpler and intuitively appealing problem of an equivalent particle moving in an effective potential according to Newton's equations of motion. This approach corresponds to the adiabatic (lowest) approximation of the perturbation theory for solitons [7]. Higher-order approximations allow us to include radiative effects accompanying the nonlinear beam scattering; the latter are important to calculate the nonlinear reflection coefficient of the light beam [8].

The purpose of the present paper is to consider analytically and numerically nonlinear dynamics of a self-trapped light beam confined or scattered by a thin-film nonlinear waveguide. We analyze the case when all media (substrate, guiding, and cladding layers) are nonlinear Kerr-like dielectrics (see Sec. II for the model description). Our analytical approach is based on the soliton phenomenology, and in Sec. III we show that this approach allows us, in a simple way, to describe bifurcations of the stationary field structures. However, we have found by numerical simulations a strong manifestation of radiation-induced effects which seem to be also very important in the beam scattering, and they cannot be taken into account by the equivalent particle theory. In particular, in Sec. IV we describe the effect of the radiation-induced capture of the scattering beam which results in a surface (guided) wave. One of the important issue of our analysis is to demonstrate applicability limits of the equivalent particle theory. At last, Sec. V concludes the paper.

II. MODEL

We consider the propagation of the TE electromagnetic wave in the symmetric waveguide structure directed along the z axis and bounded in the transverse x direction. The optical media differ by refractive indices, which we assume to be of the Kerr type. In this case the stationary field propagation is described by the slowly varying field envelope satisfying the equation

$$2i\beta\frac{\partial E}{\partial z}+\frac{\partial^2 E}{\partial x^2}-[\beta^2-n^2(x,|E|^2)]E=0, \tag{1}$$

where $E(x,z)$ stands for the electric-field envelope. The effective wave number β can be interpreted as the waveguide index. Assuming a symmetric thin-film waveguide structure, we take the refractive index as follows:

$$n^2(x,|E|^2)=n_j^2+\alpha_j|E|^2, \tag{2}$$

where $j=0$ corresponds to the guiding layer (when $|x|\le L/2$, L being the layer width) and $j=1$ to the equivalent cladding and substrate layers (when $x<-L/2$ and $x>L/2$) [see Fig. 1(a)].

After changing the variables we may reduce Eqs. (1) and (2) to the standard form of the perturbed nonlinear Schrödinger (NLS) equation for the renormalized envelope $\Phi(x,t)$ defined through the relation

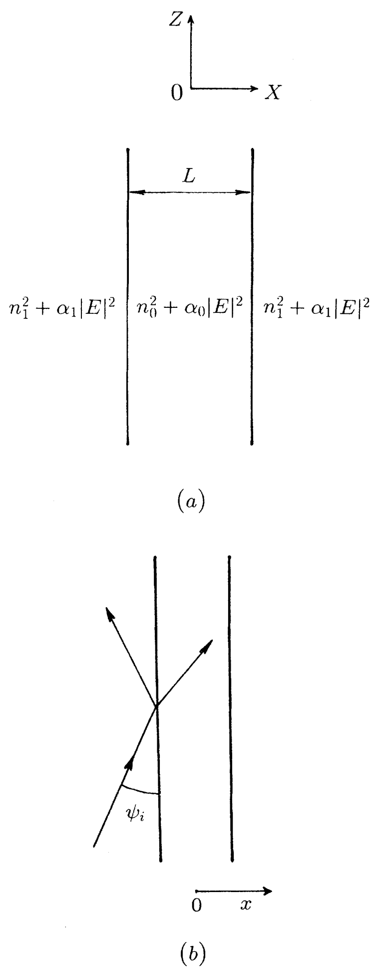

FIG. 1. (a) Sketch of the thin-film waveguide geometry. (b) Beam interaction geometry defined by the incident angle ψ_i.

$$E(x,z)=\sqrt{\frac{2}{\alpha_1}}\Phi(x,t)\exp[-i(\beta^2-n_1^2)t], \tag{3}$$

where $t=z/2\beta$. The resulting NLS equation takes the form

$$i\frac{\partial\Phi}{\partial t}+\frac{\partial^2\Phi}{\partial x^2}+2|\Phi|^2\Phi=U(x,|\Phi|^2)\Phi, \tag{4}$$

where U is the steplike potential

$$U(x)=\begin{cases}-\Delta+A|\Phi|^2 & \text{if } |x|<\frac{L}{2}\\ 0 & \text{otherwise}\end{cases} \tag{5}$$

and

$$A\equiv 2\left(1-\frac{\alpha_0}{\alpha_1}\right),\quad \Delta\equiv n_0^2-n_1^2. \tag{6}$$

Equation (4) is written as the standard NLS equation; however, it is necessary to remember that the normalized time t plays a role of the coordinate z along the waveguide.

For $U=0$, i.e., when the nonlinear medium is homogeneous, Eq. (4) has an exact solution in the form of a self-localized channel, the soliton of the NLS equation,

$$\Phi_s(x,t)=2i\mu\frac{\exp[-2i\xi x+i\delta(t)]}{\cosh\{2\mu[x-X_0(t)]\}}, \tag{7}$$

where 2μ and 4ξ define the amplitude and velocity and $\delta(t)=4(\xi^2-\mu^2)t+\delta(0)$ and $X_0(t)=-4\xi t+X_0(0)$, the phase and coordinate of the soliton, respectively. In the primary units, the velocity -4ξ of the soliton (7) appears to be proportional to the sine of the beam angle of incidence [see Fig. 1(b)]

$$\sin\psi_i=2\xi/\beta \tag{8}$$

and the soliton's amplitude 2μ to the beam power defined as

$$P=\int_{-\infty}^{+\infty}|E|^2dx=\frac{2}{\alpha_1}\int_{-\infty}^{+\infty}|\Phi|^2dx=8\mu/\alpha_1. \tag{9}$$

According to Eqs. (4) and (5), for $U\neq 0$ the waveguide geometry leads to creation of a local (for $|x|<L/2$) potential in the NLS equation which changes the dynamics of the beam (7). One of the main physically important effects is *capture* of the beam by the waveguide to create a guided (surface) wave. Stationary solutions of Eq. (1) corresponding to such surface waves have been analyzed in [5] (see also [6]). In the present paper we are mostly interesting in nonlinear dynamics of a scattering beam trying to get a deeper physical insight into the radiation-induced effects which accompany the dynamics of scattering and confined beams.

III. EFFECTIVE POTENTIAL AND BIFURCATIONS

If in the perturbed NLS equation (4) and (5) the parameters Δ and A turn out to be small, the beam dynamics in the waveguide may be analyzed by the perturbation theory for solitons [7]. For example, slow changes of the soliton parameters can be described in the framework of the so-called *adiabatic approximation*, asuming that the beam profile is still defined by the expression (7), but its parameters are changing during the scattering. The similar approach was called, in [3], *the equivalent particle theory*.

Substituting the perturbation (5) into the equations of the soliton perturbation theory [7], we obtain four equations for the soliton's parameters μ, ξ, X_0, and δ. As a matter of fact, the equation for μ is trivial and it gives $\mu = \text{const}$, but the equations for ξ and X_0 are combined to yield a single equation

$$\frac{d^2X_0}{dt^2} = -\frac{dW}{dX_0}, \tag{10}$$

which may be treated as Newton's equation for a classical particle of unit mass moving in the external potential,

$$W(X_0) = (\Delta - 2\mu^2 A)\left[\tanh S_- - \tanh S_+\right] + \frac{2}{3}\mu^2 A\left[\tanh^3 S_- - \tanh^3 S_+\right], \tag{11}$$

where

$$S_\pm \equiv 2\mu\left(X_0 \pm \frac{L}{2}\right). \tag{12}$$

Introducing the variable Z and parameters l and γ defined as

$$Z = 2\mu X_0, \quad l = \mu L, \quad \gamma = \frac{2A}{\Delta}\mu^2, \tag{13}$$

we may rewrite the effective potential (11) in the form $V(Z) = W(X_0)/\Delta$, where

$$V(Z) = (1-\gamma)\left[\tanh(Z-l) - \tanh(Z+l)\right] + \frac{1}{3}\gamma\left[\tanh^3(Z-l) - \tanh^3(Z+l)\right], \tag{14}$$

which is now defined by only two dimensionless parameters l and γ.

For small γ the potential (14) has the only minimum $V_{\min} = -2\tanh(l)$ at $Z = 0$, which corresponds to a surface wave confined just at the middle of the waveguide. When the nonlinearity parameter γ increases, new minima may appear and all different shapes of the potential $V(Z;\gamma,l)$ are defined by an interplay between two parameters l and γ.

In the case of a thin-film waveguide, the primary minimum splits via a bifurcation at which the beam position at $Z = 0$ becomes *unstable* [see Fig. 2(a)]. To analyze this bifurcation, we expand the potential (14) in small Z to find

$$V(Z) \approx V_0 + CZ^2 + DZ^4, \tag{15}$$

where

$$V_0 = -2\tanh(l)\left[(1-\gamma) + \frac{\gamma}{3}\tanh^2 l\right], \tag{16}$$

and

$$C = \frac{2\tanh l}{\cosh l}\left[1 - \frac{2\gamma}{\cosh^2 l}\right], \tag{17}$$

$$D = \frac{2\tanh l}{3\cosh^2 l}\left[1 - \frac{(3+8\gamma)}{\cosh^2 l} + \frac{15\gamma}{\cosh^4 l}\right] > 0. \tag{18}$$

As follows from Eqs. (15)–(18), when

$$\gamma < \gamma_{\text{cr}} \equiv \frac{1}{2}\cosh^2 l, \tag{19}$$

the potential (14) has a single minimum at the point $Z = 0$. However, at $\gamma = \gamma_{\text{cr}}$ ($C = 0$), a bifurcation occurs and for $\gamma > \gamma_{\text{cr}}$ two new minima appear at the points

$$Z_{1,2} = \pm\sqrt{|C|/2D}. \tag{20}$$

This bifurcation is a result of nonlinear properties of the thin-film waveguide; it naturally changes the stationary structure of a surface wave in the waveguide (see [5]). For a fixed γ the threshold value (19) determines the critical width of the slab at which the bifurcation occurs, $l_{\text{cr}} = \cosh^{-1}(\sqrt{2\gamma})$. When the normalized width is not small, say $l \gg l_{\text{cr}}$, bifurcations may be observed even earlier (for not small l), giving rise to a more complicated structure of the effective potential and the stationary points [see Fig. 2(b)].

The simple analysis shows that the bifurcations are absent for the case $A\Delta < 0$ and the effective potential is always attractive for $A < 0$ and $\Delta > 0$ and it is always repulsive for $A > 0$ and $\Delta < 0$.

As we will see from the subsequent results, the shape of the effective potential V is a very important characteristic which may be determined in the framework of the equivalent-particle theory, and this function describes rather well the transmission and reflection properties of beams as well as stationary states corresponding to guided waves. In particular, using this approach we can find, in a simple way, the conditions for the total transmission or total reflection of the beam. Indeed, the only thing we need to know for that is the maximum value of the effective potential $V_{\max} = \max\{V\}$, so that the effective particle will pass the potential provided $E_k = \frac{1}{2}(d^2X_0/dt^2) > V_{\max}$. Using such a consideration, we can evaluate the required initial velocities of the particle (i.e., in fact, the angles of incidence for the beam) corresponding to the total beam transmission or reflection.

To investigate the transmission and reflection numerically, we solve Eqs. (4) and (5) by the well-known split-step Fourier transform method [9]. The beam parameters are defined as the coordinate of the centrum of mass and velocity of the effective particle, respectively, by using the following relation:

$$X_0 = \int_{-\infty}^{+\infty} x\,|\Phi|^2\,dx \bigg/ \int_{-\infty}^{+\infty} |\Phi|^2\,dx \tag{21}$$

and $4\xi \approx -\dot{X}_0$ for the particle's velocity. One of the important characteristics of the beam scattering is the critical angle of the beam reflection which corresponds to the critical velocity of the equivalent particle. We have determined this value from the energy balance given by the equivalent-particle theory and also by means of numerical simulations. The comparison of the results is shown in Figs. 3(a) and 3(b) where such a dependence separates regions of reflection and transmission for the equivalent particle (shown as insert pictures in the plots). It is important to note that the numerical data presented by full circles are *below* the corresponding values following from the results of the equivalent particle approach, and this clearly indicates that the energy balance equations have to be corrected to include a part of the particle's energy lost in such a scattering. As a matter of fact, such a correction is nothing but radiation-induced losses, which are not taken into account by the equivalent particle theory.

Another type of the beam dynamics in the nonlinear waveguides which may be treated by tools of the equivalent-particle approach is the *beam amplification* in the so-called active guides when there is a gain in the wave-guide or in the guiding film [10]. The simplest problem is a homogeneous gain, which is described by the term $ig\Phi$ in Eq. (4), g being the gain parameter. In this case the intensity integral $\int |\Phi|^2 dx = N$ is not conserved anymore, and its evolution is described by the exact relation $dN/dt = gN$, i.e., the pulse power is growing exponentially with the increment g. Let us treat the gain effect as small; the latter means that the gain-induced evolution of the beam is assumed to be slower that other types of the beam dynamics. Then, from the equation for the total beam intensity it follows the evolution equation for the amplitude μ, $\mu = \mu(0)\exp(gt)$. Now, assuming in the equations of the equivalent-particle approach that the parameter μ is *slowly dependent* on time, we may obtain the conclusion that the main effect produced by the gain is *to deform the shape of the effective potential* according, e.g., to the set of the plots shown in Fig. 2(a) or 2(b). For the case $A > 0$ and $\Delta > 0$, we obtain that the potential changes crossing the bifurcation point where the symmetric structure becomes unstable. Figure 4(a) shows the case of a thin-film waveguide where the evolution of the effective potential corresponds to the case shown in Fig. 2(a). We can see how the beam is displaced to one of the sides due to that bifurcation. For large values of l the potential is changing, but it remains stable in the vicinity of the point $Z = 0$, so that the amplified beam is also stable [see Fig. 4(b)].

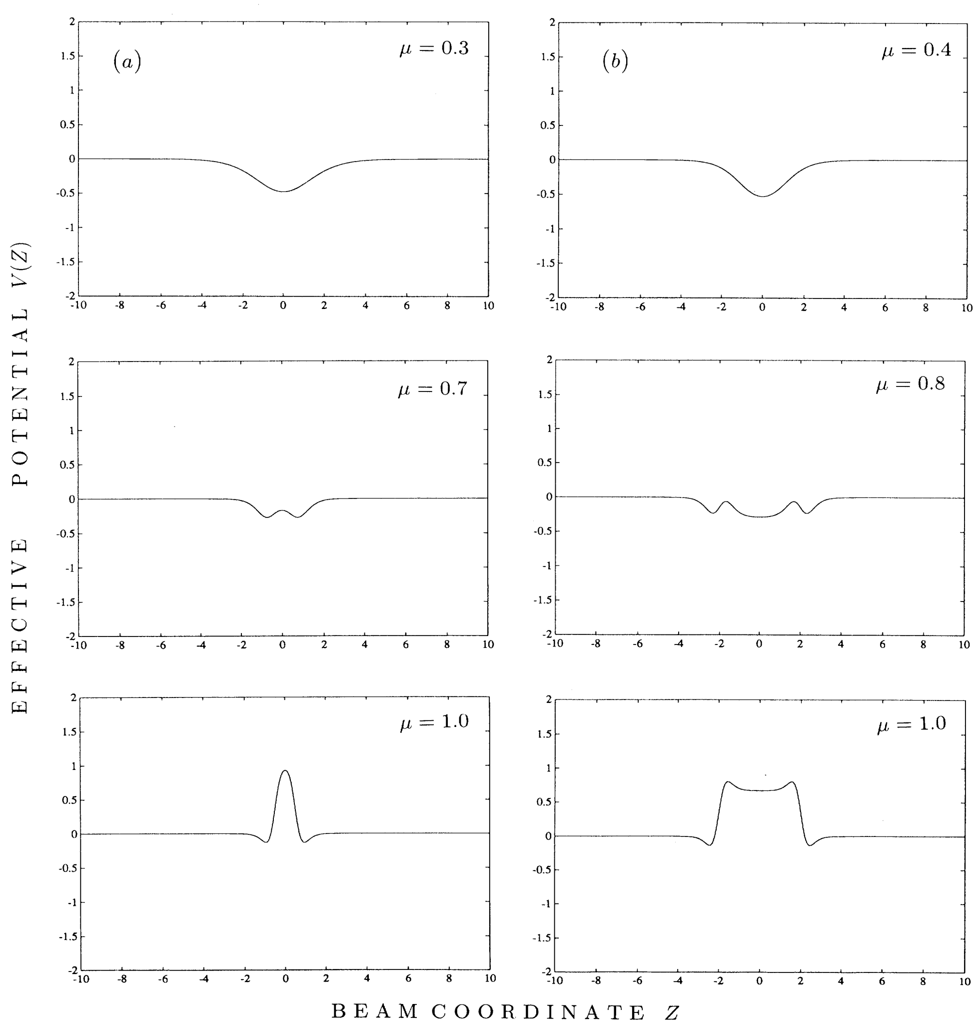

FIG. 2. Shapes of the effective potential V for $A > 0$ and $\Delta > 0$: (a) a thin-film waveguide ($L = 1.0$, $A = \Delta = 0.1$), and (b) a wide waveguide ($L = 4.0$, $A = \Delta = 1.0$). The beam intensity is measured by the parameter μ.

IV. RADIATION-INDUCED EFFECTS

The slow change of the beam parameters can be described in the framework of Eqs. (10) and (11). This approach may be considered as the first step of the regular expansions of the soliton perturbation theory [7], but the next step is to calculate the first-order correction to the adiabatic dynamics, which consists of the contributions of two types: the first type corresponds to a distortion of the beam shape and the second type is the dispersive wave packets propagating in both direction (reflected and transmitted radiation). The simplest way to estimate the radiation-induced losses at the beam scattering is to use the soliton perturbation theory [7] based on the inverse scattering transform (IST) [11]. According to the IST, the total intensity of the radiation emitted at the moment t is given by the expression

$$N = \int_{-\infty}^{+\infty} |\Phi|^2 dx = \int_{-\infty}^{+\infty} n(\lambda, t) d\lambda, \tag{22}$$

where the spectral density $n(\lambda, t)$ may be calculated in the framework of the IST throught the so-called Jost coefficient $b(\lambda, t)$, $n(\lambda, t) = -\frac{1}{\pi} \ln |a(\lambda, t)|^2 = -\frac{1}{\pi} \ln(1 - |b(\lambda, t)|^2) \simeq \pi^{-1} |b(\lambda, t)|^2$. The spectral parameter λ appearing in the IST is connected with the wave number $k(\lambda)$ and the frequency $\omega(\lambda)$ of the generated linear waves for which the dispersion relation $\omega(\lambda) = k^2 = 4\lambda^2$ is

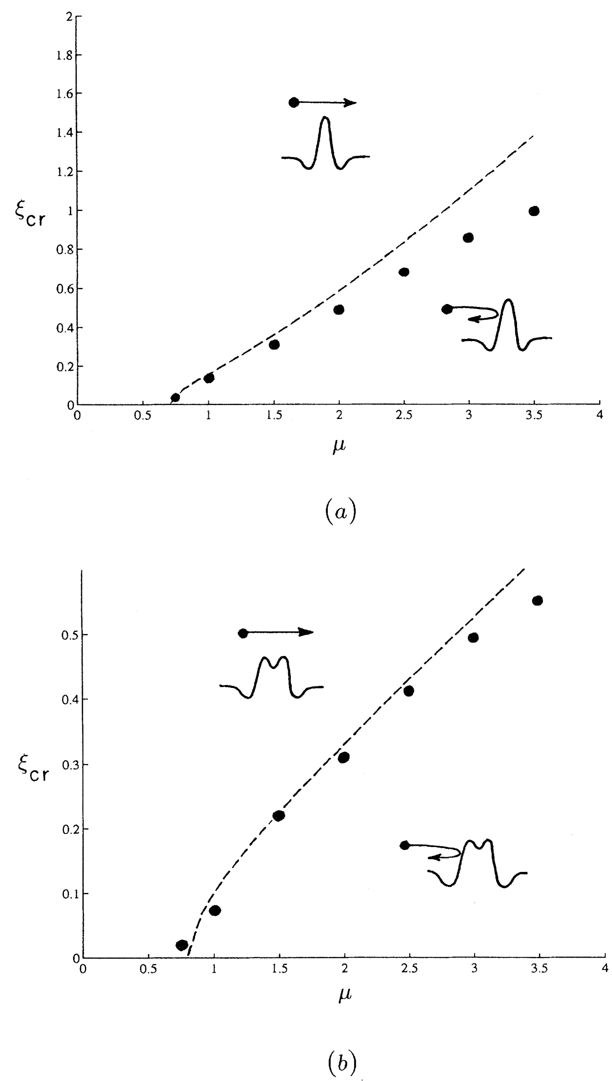

FIG. 3. The critical value for the normalized angle of incidence (particle's velocity) for the beam transmission-reflection vs the beam intensity. The dashed line shows the result of the equivalent particle approach and the full circles are given by results of numerical simulations which use the formula $4\xi \approx -\dot{X}_0$, where X_0 is defined with the help of Eq. (21): (a) $A = 1.0$, $\Delta = 1.0$, and $L = 0.1$; and (b) $A = 0.1$, $\Delta = 0.1$, and $L = 2.0$. Note that for these two sets of the parameters the ratio A/Δ is the same.

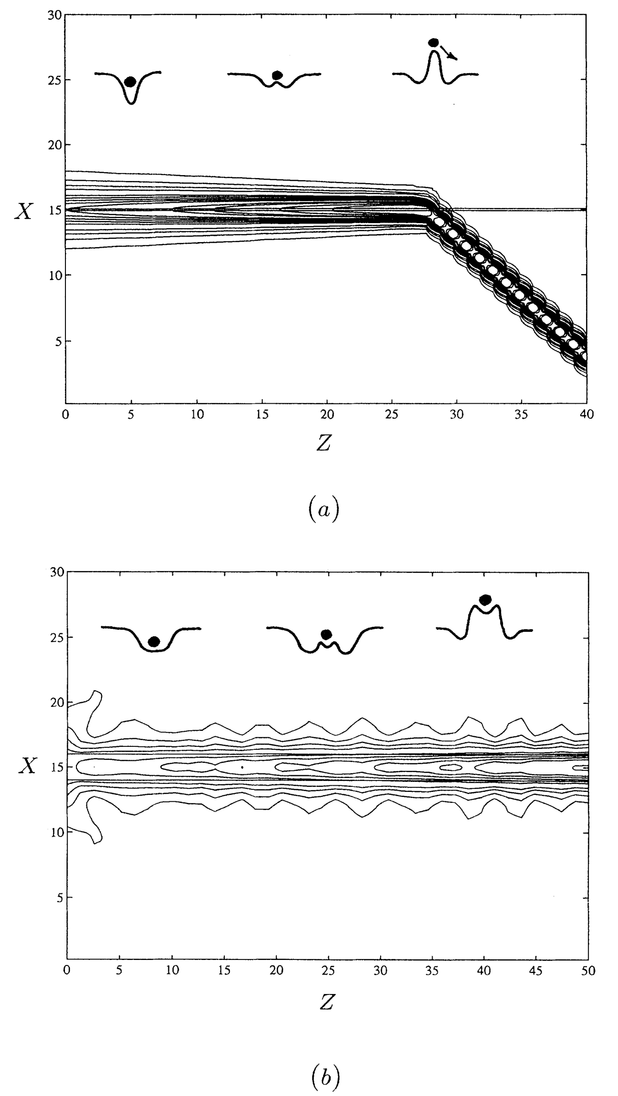

FIG. 4. Beam evolution in the amplified guide at $g = 0.001$ for (a) $\mu = 0.5$ and $L = 0.1$, and (b) $\mu = 0.25$ and $L = 2.0$. The cases (a) and (b) correspond, respectively, to two different cases of the potential shape evolution shown in Figs. 2(a) and 2(b), respectively.

valid. The influence of the perturbation (5) leads to a change of the IST spectral parameters including the Jost coefficient $b(\lambda, t)$. If prior to the scattering the beam corresponds to a soliton, the initial condition for the equation describing the evolution of the $b(\lambda, t)$ may be taken as $b(\lambda, t = -\infty) = 0$. Then the total intensity of the emitted radiation is given by the relation

$$N = \int_{-\infty}^{+\infty} n(\lambda) d\lambda = \frac{1}{\pi} \int_{-\infty}^{+\infty} n(\lambda, t = +\infty) d\lambda. \tag{23}$$

The details of the method discussed may be found in Refs. [7, 8, 12], but here we will give only the final result for the total intensity which is lost due to radiation of linear waves,

$$N_{\text{rad}} = \frac{\pi}{2^6 \xi^4} \int_{-\infty}^{+\infty} dy\, G^2(y, \alpha) \frac{\sin^2\left(\frac{d}{2}[(y-1)^2 + \alpha^2]\right)}{\cosh^2\left(\frac{\pi}{2\alpha}(y^2 + \alpha^2 - 1)\right)}, \tag{24}$$

where

$$G(y, \alpha) = \left[\Delta - \frac{A\mu^2}{3}\left(1 + \frac{(y^2 + \alpha^2 - 1)^2}{4\alpha^2}\right)\right] \times \left[1 + \frac{4(4 - y)}{[(y-1)^2 + \alpha^2]}\right], \tag{25}$$

and $d \equiv L\xi$. The result (25) is useful to estimate the radiation-induced reflection coefficient of the beam, and the similar results for one and two interfaces may be found in [8]. One of the most important radiation-induced effects is a trapping of the beam into a surface wave due to radiation. This process is characterized by a threshold value of the soliton velocity (i.e., a threshold value of the beam angle of incidence, in the primary units). This threshold value may be found with the help of simple physical estimates, for which we use the conservation laws of the power N and the system energy

$$E = \int_{-\infty}^{+\infty} [|\Phi_x|^2 - |\Phi|^4 - U(x)|\Phi|^2] dx. \tag{26}$$

Let us suppose that a soliton has a low velocity (angle) $\xi = \xi_0$ at $t = -\infty$. After the scattering, i.e., for $t = +\infty$, we assume that the soliton is captured, so that the energy of the full system contains, besides the energy of the soliton at rest, the contribution of the radiated energy carried away by linear waves. Therefore, we may write $16(\xi_0^2\mu - \frac{1}{3}\mu^3) = E_{\text{rad}} - \frac{16}{3}(\mu + \delta\mu)^3$, where the left-hand side is the energy of the soliton with the amplitude 2μ and the velocity 4ξ and we have assumed that the soliton changes its amplitude after the scattering in the value $\delta\mu$. From the power conservation it follows that $4\mu = 4(\mu + \delta\mu) + N_{\text{rad}}$, where N_{rad} has to be calculated in the limit $\xi_0 \to 0$. It may be proved that the kinetic energy E_{rad} is much smaller than N_{rad}, so that we may omit E_{rad} in the first relation to get the threshold value ξ_* for the beam trapping

$$\xi_*^2 \simeq \frac{1}{4}\mu N_{\text{rad}}. \tag{27}$$

The result (27) determines the threshold angle of incidence ψ_* for the beam trapping,

$$\sin^2 \psi_* = \frac{\mu}{\beta^2} N_{\text{rad}}. \tag{28}$$

In fact, to use the result (27) for an analytical estimation of a critical angle ψ_*, we have to calculate N_{rad} in the limit when the soliton (beam) has a zero velocity prior to the scattering, and its evolution is described by the equivalent particle approach, i.e., Newton's equations.

Radiation-induced trapping of the beam into a surface wave can be easily analyzed numerically. We take the case $A = -1.0$ and $\Delta = 1.0$ when the effective potential $V(Z)$ is always attractive (for any l) and these values are not small to make the radiation-induced effects more observable. The contour plot corresponding to the numerical simulation of the beam trapping is shown in Fig. 5(a) where the formation of a surface wave through the process of a strong emission of radiation may be clearly seen. This effect may be also analyzed by studing evolution of the beam coordinate X_0 calculated numerically with the help of the formula (21), and the corresponding phase plane is shown in Fig. 5(b). The phase plane $(X_0, \dot{X}_0)$ looks like that for a particle moving in an attractive potential under the action of a friction force. Thus the equivalent-particle approach is still useful to characterize different types of the beam scattering, but the theory has to be modified by inclusion of an effective dissipation which takes into account radiation-induced losses.

To calculate the critical velocity ξ_* analytically, in the general formula for the radiation power we have to take into account the evolution of particle's velocity during the scattering that follows from the equations of the equivalent-particle approach. This may be done only in a few particular cases, e.g., for a very thin linear slab when $A = 0$, but $L \to 0$, $\Delta \to \infty$ keeping the product $L\Delta = \epsilon$ unchanged. In this latter case the motion equation for the effective particle with $\dot{X}_0(-\infty) = 0$ may be easily integrated to yield the result $X_0 = -(1/2\mu)\sinh^{-1}(4\mu\sqrt{\mu t})$, and the value N_{rad} is calculated to be exponentially small [12]

$$N_{\text{rad}} = \frac{\sqrt{\pi}}{4\sqrt{2}}\mu\left(\frac{\epsilon}{\mu}\right)^{3/4} \exp\left(-2\sqrt{\frac{\mu}{\epsilon}}\right).$$

In a general case the value N_{rad} may be found numerically, e.g., by measuring the beam power lost through emission of radiation. To calculate this value numerically, we use the nonlinear spectral analysis based on the IST to the NLS equation [11]. We solve the Zakharov-Shabat (ZS) eigenvalue problem numerically at each point of z taking the beam profile as an effective potential in the matrix method proposed in [13]. From that numerical analysis we obtain the parameters μ and ξ of the soliton as a position of the complex eigenvalue $\lambda_1 = \xi + i\mu$, where λ_1 is a solution of the equation $a(\lambda_1) = 0$, $a(\lambda)$ being the so-called Jost coefficient of the IST method. The intensity of the radiation is calculated by using the well-known formula of the IST method,

$$N_{\text{rad}} = -\frac{1}{\pi}\int_{-\infty}^{\infty} \ln|a(\lambda)|^2\, d\lambda.$$

The numerical results obtained with the help of the ZS eigenvalue problem are shown in Fig. 5(c) where $N_{\rm sol} = 4\,{\rm Re}\lambda_1$. As may be seen in Fig. 5(c), the process of the radiation-induced trapping of the beam by a thin-film waveguide may be treated as a transformation of the kinetic energy of the equivalent particle into radiation ($N_{\rm rad}$). If, however, we take larger angles of the incidence (as it is shown in Fig. 6), the strong emission of radiation is still clearly observed, but it is not enough to support the trapping (see Fig. 6). The dependence of the critical particle velocity (i.e., the critical angle of incidence for the beam) ξ_* vs the beam intensity characterized by the parameter μ has been determined numerically, and the result is shown in Fig. 7 where the region under the solid curve corresponds to the beam trapping by the slab. As may be seen from Fig. 7, the value ξ_* is not small for the selected values of the waveguide parameters and it displays a maximum at $\mu \approx 2.5$. These numerical results are in a good qualitative agreement with Eq. (27) if we will treat the value $N_{\rm rad}$ in Eq. (27) as a result of numerical simulations.

V. CONCLUSIONS

In conclusion, we have investigated analytically and numerically the light-beam propagation at a symmetric

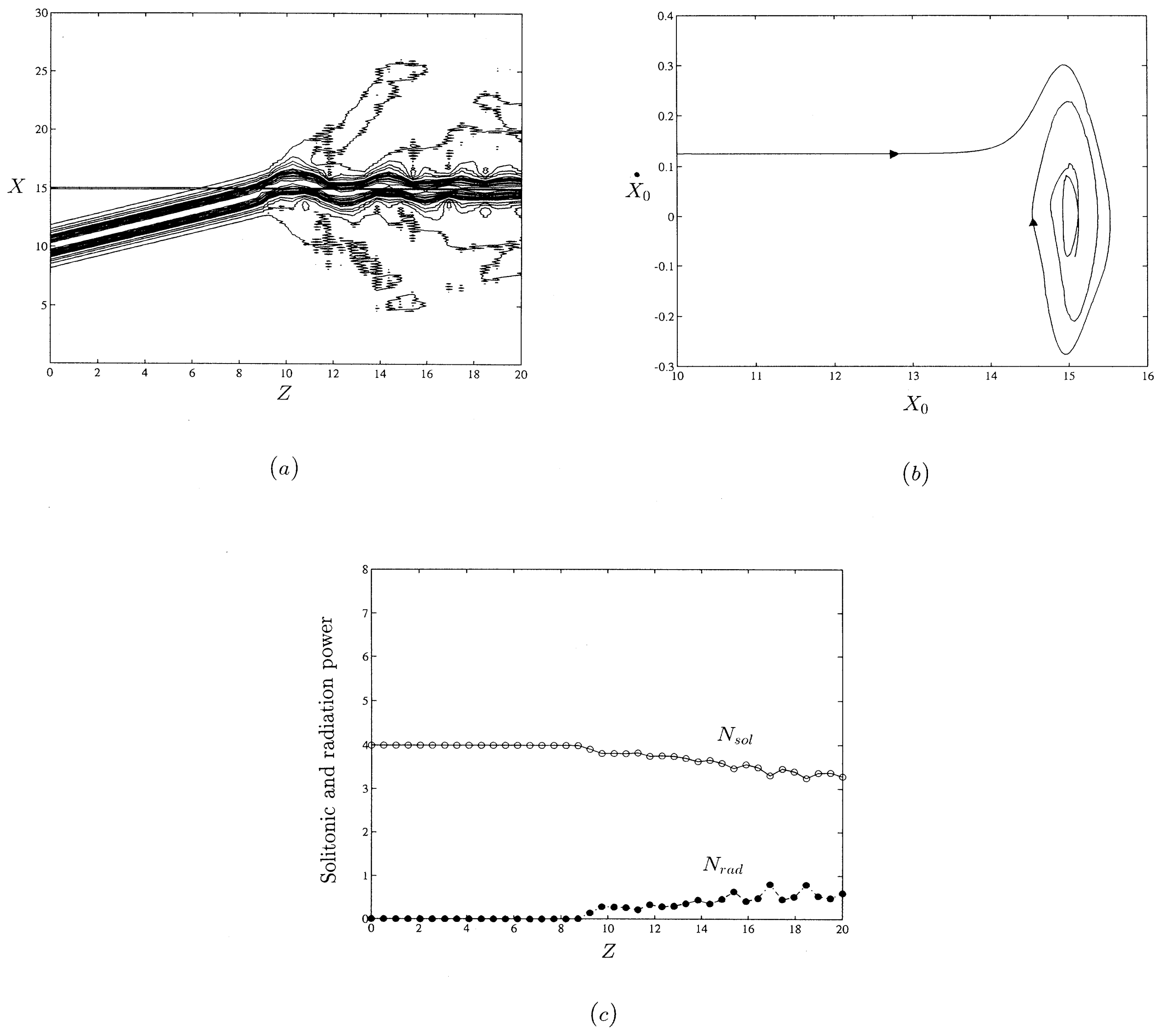

FIG. 5. Radiation-induced trapping of the beam by the waveguide slab. The parameters of the waveguide are $A = -1.0$, $\Delta = 1.0$, and $L = 0.1$, whereas the parameters of the incident beam are taken to be $\mu = 1.0$ and $\xi_0 = 0.125$. (a) Contour plot for the beam intensity. (b) The phase plane for the beam parameters defined with the help of the formula (21). (c) Evolution of the intensity of the solitonic ($N_{\rm sol}$) and radiation ($N_{\rm rad}$) components defined by a numerical solution of the Zakharov-Shabat eigenvalue problem.

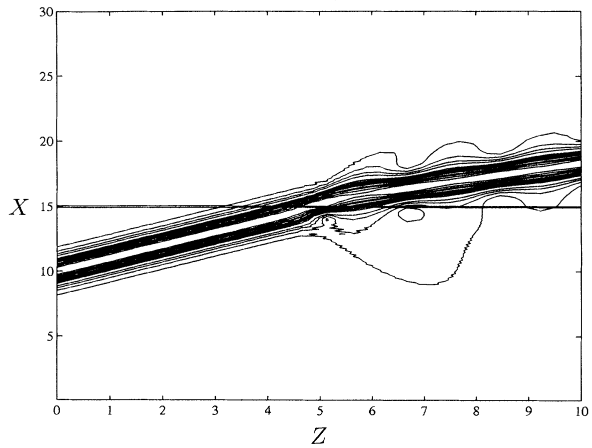

FIG. 6. The same as in Fig. 5(a), but for $\xi_0 = 0.25$. The beam passes the waveguide slab, but radiative losses are clearly observed. Note that the scales of Fig. 5(a) and this figure are different.

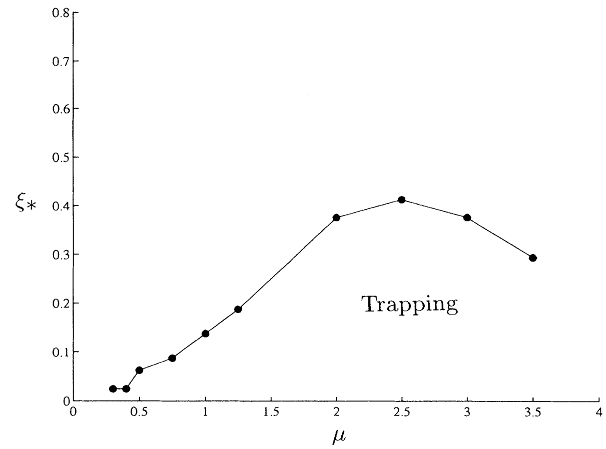

FIG. 7. The threshold value ξ_* of the normalized angle of incidence (velocity of the effective particle) for the radiation-induced beam trapping vs the beam intensity parameter μ. The waveguide parameters are the same as in Fig. 5. The results of numerical simulations are consistent with Eq. (27) provided that the value $N_{\rm rad}$ is found from numerical simulations [see, e.g., Fig. 5(c)].

dielectric waveguide formed by two interfaces between three nonlinear self-focusing media. As has been shown, the critical characteristics of the transmission and reflection may be found in the framework of the equivalent particle approach that has been checked to be a rather good approximation to calculate, e.g., the critical angle of the beam reflection. However, we have observed that the beam scattering at small angles of incidence is accompanied by emission of radiation which is stronger for the case $A\Delta < 0$ than for the case $A\Delta > 0$. We have pointed out that such a radiation is indeed responsible for the beam trapping into a surface wave, and we have determined analytically and numerically the threshold angle characterizing such an effect. We believe that the analysis and numerical simulations presented allow us to display the validity limits of the equivalent-particle theory. As a matter of fact, in many cases we have investigated, the beam scattering may still be characterized by motion of a particle in an effective potential, but this motion is modified by a friction due to emission of radiation.

ACKNOWLEDGMENTS

Y.S.K. thanks J. Moloney for fruitful discussions and useful suggestions. His work was supported by the Alexander von Humboldt Stiftung. He is also indebted to V. Shekhter for his help at the initial stage of this work. M.L.Q.-T. acknowledges the financial support of the Ministerio de Asuntos Exteriores de España and the Swedish Technical Board.

* Present address: Optical Sciences Center, Australian National University, Australian Capital Territory 2601, Canberra, Australia.

[1] A.D. Boardman, P. Egan, T. Twardowski, and M. Wilkins, in *Nonlinear Waves in Solid State Physics*, edited by A.D. Boardman *et al.* (Plenum, New York, 1990).
[2] J.V. Moloney and A.C. Newell, Physica D **44**, 1 (1990).
[3] A.B. Aceves, J.V. Moloney, and A.C. Newell, Phys. Lett. A **129**, 231 (1988); J. Opt. Soc. Am. B **5**, 559 (1988); Phys. Rev. A **39**, 1809 (1989); **39**, 1828 (1989).
[4] W.J. Tomlison, J.P. Gordon, P.W. Smith, and A.E. Kaplan, Appl. Opt. **21**, 2041 (1982).
[5] N.N. Akhmediev, Zh. Eksp. Teor. Fiz. **83**, 545 (1982) [Sov. Phys. JETP **56**, 299 (1982)].
[6] C.S. Mitchel and J.V. Moloney, Opt. Commun. **69**, 243 (1989).
[7] Yu.S. Kivshar and B.A. Malomed, Rev. Mod. Phys. **61**, 763 (1989).
[8] Yu.S. Kivshar, A.M. Kosevich, and O.A. Chubykalo, Phys. Rev. A **41**, 1677 (1990).
[9] D. Yevick and B. Hermansson, Opt. Commun. **47**, 101 (1983).
[10] N. Akhmediev, N. Mitskevich, and R. Nabiev, Phys. Rev. A **45**, 2006 (1992).
[11] V.E. Zakharov and A.B. Shabat, Zh. Eksp. Teor. Fiz. **61**, 118 (1971) [Sov. Phys. JETP **34**, 62 (1972)].
[12] Yu.S. Kivshar, A.M. Kosevich, and O.A. Chubykalo, Zh. Eksp. Teor. Fiz. **93**, 968 (1987) [Sov. Phys. JETP **66**, 545 (1987)].
[13] V.V. Afanasjev, V.N. Serkin, and V.A. Vysloukh, Sov. Ligh. Comm. **2**, 35 (1992).